OPEN

Grainyhead-like 2 Deficiency and Kidney Cyst Growth in a Mouse Model

Zeliha Yesim Yurtdas[1,2,3] *Ergin Kilic*[4] *Peter Boor*[5] *Emanuel Wyler*[6] *Markus Landthaler*[6,7] *Klaus Jung*[2,3] *and Kai M. Schmidt-Ott*[1,8,9]

Key Points

- Our study reveals segment-specific mechanisms in cystic kidney disease and suggests *Grhl2* as a modifier of collecting duct–derived cyst progression.
- Our data demonstrate that genetic deletion of *Grhl2* accelerates disease progression in a cystic mouse model.

Abstract

Background The transcription factor grainyhead-like 2 (GRHL2) plays a crucial role in maintaining the epithelial barrier properties of the kidney collecting duct and is important to osmoregulation. We noticed a reduction in GRHL2 expression in cysts derived from the collecting ducts in kidneys affected by autosomal dominant polycystic kidney disease (ADPKD). However, the specific role of GRHL2 in cystic kidney disease remains unknown.

Methods The functional role of the transcription factor Grhl2 in the context of cystic kidney disease was examined through analysis of its expression pattern in patient samples with ADPKD and generating a transgenic cystic kidney disease (TCKD) mouse model by overexpressing the human proto-oncogene *c-MYC* in kidney collecting ducts. Next, TCKD mice bred with collecting duct–specific *Grhl2* knockout mice (Grhl2KO). The resulting TCKD-*Grhl2*KO mice and their littermates were examined by various types of histological and biochemical assays and gene profiling analysis through RNA sequencing.

Results A comprehensive examination of kidney samples from patients with ADPKD revealed GRHL2 downregulation in collecting duct–derived cyst epithelia. Comparative analysis of TCKD and TCKD-*Grhl2*KO mice exhibited that the collecting duct–specific deletion of *Grhl2* resulted in markedly aggravated cyst growth, worsened kidney dysfunction, and shortened life span. Furthermore, transcriptomic analyses indicated sequential downregulation of kidney epithelial cyst development regulators (*Frem2*, *Muc1*, *Cdkn2c*, *Pkd2*, and *Tsc1*) during cyst progression in kidneys of TCKD-*Grhl2*KO mice, which included presumed direct *Grhl2* target genes.

Conclusions These results suggest Grhl2 as a potential progression modifier, especially for cysts originating from collecting ducts.

JASN 35: 838–853, 2024. doi: https://doi.org/10.1681/ASN.0000000000000353

[1]Molecular and Translational Kidney Research, Max-Delbrück Center for Molecular Medicine in the Helmholtz Association, Berlin, Germany
[2]Berlin Institute for Urologic Research, Berlin, Germany
[3]Department of Urology, Charité - Universitätsmedizin Berlin, Corporate Member of Freie Universität Berlin and Humboldt-Universität zu Berlin, Berlin, Germany
[4]Medical School Hamburg, Department of Pathology, Hamburg, Germany
[5]Institute of Pathology and Department of Nephrology, University Hospital of the RWTH Aachen, Aachen, Germany
[6]Berlin Institute for Medical Systems Biology, Max-Delbrück-Center for Molecular Medicine in the Helmholtz Association, Berlin, Germany
[7]Institute für Biologie, Humboldt-Universität zu Berlin, Berlin, Germany
[8]Department of Nephrology and Medical Intensive Care, Charité - Universitätsmedizin Berlin, Corporate Member of Freie Universität Berlin and Humboldt-Universität zu Berlin, Berlin, Germany
[9]Department of Nephrology and Hypertension, Hannover Medical School, Hannover, Germany

Correspondence: Dr. Kai M. Schmidt-Ott, email: Schmidt-Ott.Kai@mh-hannover.de

Received: April 1, 2023 **Accepted:** April 8, 2024
Published Online Ahead of Print: April 24, 2024

Introduction

Polycystic kidney disease (PKD) encompasses a diverse range of disorders, which may result from hereditary inheritance, adult-onset acquisition, or sporadic developmental abnormalities. Among the various inherited forms, autosomal recessive PKD (ARPKD) and autosomal dominant PKD (ADPKD) are the most prevalent types.[1] ARPKD is a rare and lethal form of PKD characterized by the expansion and elongation of collecting duct tubules that result in multiple cysts in both kidneys. Mutations in the *PKHD1* gene, which encodes fibrocystin/polyductin protein, is the genetic cause of ARPKD.[2] ADPKD is the most prevalent, potentially lethal, Mendelian human disorder,[3] a condition with related but distinct pathogeneses characterized by the development of kidney cysts and various extrarenal manifestations. In ADPKD, the phenotypes also include cysts in other organs, such as the liver, seminal vesicles, pancreas, and arachnoid membrane, as well as other abnormalities, such as intracranial aneurysms, dolichoectasias, aortic root dilatation, mitral valve prolapse, and abdominal wall hernias.[4] ADPKD belongs to the ciliopathies. The glycoprotein polycystin-1, encoded by *PKD1*, is present on the renal cilia and is believed to sense filtrate flow with large extracellular domains that include activating calcium channels associated with another glycoprotein polycystin-2, encoded by *PKD2*. Organ destruction occurs through continuous cyst growth that may involve cAMP generation promoting fluid entry through transepithelial secretion.[5] Cyst growth can be precisely monitored clinically with magnetic resonance imaging.[4] The variable and heterogeneous cyst growth progression indicates that other modifying factors are involved in ADPKD.[6]

Grainyhead-like genes are a family of highly conserved transcription factors. They are involved in epithelial barrier formation, wound healing, and various critical developmental processes. Grainyhead-like 2 (Grhl2), encoded by *Grhl2*, is not only important to craniofacial development but also to epithelial apical junction regulation, trophoblast branching, and tubular lumen expansion.[7–9] Our group recognized the fact that Grhl2 is required for collecting duct epithelial barrier function and renal osmoregulation.[10] Thus, the importance of grainyhead-like transcription factors in kidney development and function is readily apparent.[11] The sole effective pharmacological treatment for ADPKD to date is to diminish the effect of arginine vasopressin, causing the patients to excrete dilute urine.[12] Because renal osmoregulation might be important to ADPKD, we inspected the expression of GRHL2 in samples of patients with ADPKD.

Methods

Human Kidney Samples

The ethical committees of the Universitätsmedizin Berlin (EA1/134/12) by the Declaration of Helsinki and the Institute of Pathology of the University Hospital in Aachen (EK 244-14, EK 04217) approved the studies and written informed consent to use the obtained formalin-fixed paraffin-embedded specimens from normal human kidney and patients with ADPKD (Table 1).

Table 1. Clinical characteristics of patient samples with autosomal dominant polycystic kidney disease

ADPKD Samples' ID	Age	Sex
11_10640	51	Female
E15-28591	64	Male
E16-05780	41	Male
E16-14155	40	Male
E17-14350	51	Male
11_6245	53	Male

ADPKD, autosomal dominant polycystic kidney disease.

Generation and Characterization of Transgenic Cystic Kidney Disease and Transgenic Cystic Kidney Disease–*Grhl2* Knockout Mice

Animal investigations were approved by Berlin regulatory agencies under the license numbers G0232/13 and X9001/14 according to principles outlined by the American Physiological Society. R26StopFLMYC mice, [13] from whence transgenic cystic kidney disease (TCKD) mice were generated, were a gift from Prof. Klaus Rajewsky at the Max Delbrück Center. To generate HoxB7-Cre; R26StopFLMYC (referred as TCKD), HoxB7-Cre mice bred with R26StopFLMYC. TCKD mice were born at the expected Mendelian ratios (48% TCKD and 52% R26StopFLMYC [referred to as control], 88 mice in total) and healthy but became physically ill, *i.e.*, weight loss associated with smaller body size and slow movement compared with littermate controls, by 12 weeks of age. Therefore, the kidney phenotype of *c-MYC* overexpressing mice was determined by analyzing the 10-week-old TCKD mice compared with littermate controls (Table 2).

To generate TCKD-*Grhl2* knockout (Grhl2KO) mice, the previously generated collecting duct–specific Grhl2KO mice; HoxB7-Cre; $Grhl2^{flox/flox}$ (referred as Grhl2KO),[10] crossed with R26StopFLMYC; $Grhl2^{flox/flox}$ mice. The resulting HoxB7-Cre; R26StopFLMYC; $Grhl2^{flox/flox}$ (referred as TCKD-*Grhl2*KO) mice were born at expected Mendelian ratios (32% TCKD-*Grhl2*KO; 30% HoxB7-Cre; R26StopFLMYC; $Grhl2^{flox/+}$ [referred as TCKD], 38% R26StopFLMYC; $Grhl2^{flox/flox}$ [referred as control] in total 100 mice in total). TCKD-*Grhl2*KO mice were born healthy but became severely ill, *i.e.*, weight loss associated with smaller body size and slow movement compared with littermate controls, between 4 and 6 weeks of age. Therefore, the phenotype of TCKD-*Grhl2*KO mice was determined by analyzing 5-week-old TCKD-*Grhl2*KO compared with littermate controls (Table 3).

Mouse genotyping was performed from tissues that were collected from either ears or tails; first, DNA was isolated, and then, PCR was performed with primers (Supplemental Table 1), which are standard. Mice were euthanized by ether inhalation at the indicated age (Tables 2 and 3). Then, body weights were measured, followed by removal of the left/right kidneys and measurement of kidney weights. Blood was obtained by cardiac puncture and collected into sodium-heparin–coated tubes, and then, 90 μl of blood was loaded into the CHEM8+ cartridges (09P31-25, Abbott) of Abbott-i-STAT blood analyzer to measure BUN and creatinine.

Table 2. Analyzed 10-week-old mice data from the indicated genotypes

ID	Sex	Age, wk	Mutation	Kidney Phenotype	BW, g	LKW, mg	RKW, mg	2KWs/BW, mg/g	BUN, mg/dl	Creatinine, mg/dl
KSX-06590	F	10.3	HoxB7-Cre; R26StopFLMYC	Many cysts	17	294	200	29.08	47.62	0.26
KSX-06099	F	10.6	HoxB7-Cre; R26StopFLMYC	Many cysts	14	110	112	15.85	29.4	0.21
KSX-06589	F	10.3	HoxB7-Cre; R26StopFLMYC	Many cysts	20.1	146	157	15.10	33.33	0.23
KSX-06585	M	10.3	HoxB7-Cre; R26StopFLMYC	Many cysts	14.4	115	122	16.44	24.65	0.21
KSX-05878	M	10.4	HoxB7-Cre; R26StopFLMYC	Many cysts	15	201	226	28.43	27.7	0.20
KSX-10427	F	10.3	HoxB7-Cre; R26StopFLMYC	Many cysts	12.8	121	120	18.83	28.01	0.21
KSX-10428	F	10.3	HoxB7-Cre; R26StopFLMYC	Many cysts	13.3	158	160	23.91	41.74	0.25
KSX-05876	F	10.3	HoxB7-Cre; R26StopFLMYC	Many cysts	13.2	120	130	18.94	78.15	0.27
KSX-07157	F	10.3	HoxB7-Cre; R26StopFLMYC	Many cysts	14.3	114	118	16.22	31.65	0.24
KSX-06100	F	10.6	HoxB7-Cre; R26StopFLMYC	Many cysts	16.5	130	134	16.00	26.33	0.21
KSX-05879	M	10.4	R26StopFLMYC	Normal	24.8	165	162	13.18	19.61	0.19
KSX-06584	M	10.3	R26StopFLMYC	Normal	20	140	142	14.10	18.18	0.19
KSX-06591	F	10.3	R26StopFLMYC	Normal	24.3	148	154	12.43	19.33	0.19
KSX-05877	F	10.4	R26StopFLMYC	Normal	20.6	117	135	12.22	19.33	0.20
KSX-05875	F	10.4	R26StopFLMYC	Normal	23.2	148	140	12.43	19.61	0.19
KSX-04676	F	10.3	R26StopFLMYC	Normal	18.8	112	125	12.61	18.21	0.19
KSX-06591	F	10.3	R26StopFLMYC	Normal	24.3	148	154	12.43	17.37	0.19
KSX-06433	F	10.1	R26StopFLMYC	Normal	14.6	100	102	13.82	19.61	0.19
KSX-06434	F	10.1	R26StopFLMYC	Normal	17.9	108	110	12.17	18.49	0.19
KSX-05304	M	10.7	R26StopFLMYC	Normal	20.1	119	111	11.46	19.05	0.20

HoxB7-Cre; R26StopFLMYC referred as transgenic cystic kidney disease and R26StopFLMYC referred as control. BW, body weight; F, female; ID, mouse identification number; LKW, left kidney weight; M, male; RKW, right kidney weight.

Histological Analysis of Kidney Specimens from the Generated Mouse Models

Histology was performed with standard methods at 5 μm thick sections from the prepared formalin-fixed paraffin-embedded blocks. These tissue samples were stained using conventional techniques such as periodic acid–Schiff, hematoxylin and eosin, or other staining techniques. Immunohistochemistry and immunofluorescence staining methodology involved commercial antibodies (Supplemental Tables 2 and 3). For image acquisition and analysis, samples of interests (n=3, biological replicates for each transgenic and control mice) for each experiment were prepared at the same time with the same staining conditions. The images were taken using identical image acquisition settings. Image acquisition was standardized (Leica Microsystems). We assayed cell proliferation with standardized techniques relying on Ki67 immunofluorescence staining.

Protein Isolation, SDS-PAGE, and Western Blotting

Protein isolation was performed on flash-frozen kidneys using standard techniques, with samples collected from at least n=3 biological replicates for each transgenic and control mice. We relied on SDS-PAGE, Western blotting. Full scans and band intensity analysis are shown in Supplemental Figure 2. Commercial antibodies used for Western blotting are available in Supplemental Tables 2 and 3.

RNA Extraction, cDNA Synthesis, and Real-Time Quantitative PCR

RNA extraction and cDNA synthesis, as well as real-time quantitative PCR (RT-qPCR), are standard methods. For cDNA synthesis, 500 ng RNA were reverse-transcribed into cDNA using the RevertAid First-Strand cDNA synthesis kit K1621, Thermo Fisher Scientific. We relied on RT-qPCR with 96-well plates. Based on each experiment, we used at least n=3 biological replicates for each transgenic and control mice. The primers (Supplemental Table 4) are standard.

RNA-Sequencing Library Preparation

RNA-sequencing (RNA-seq) libraries were prepared using the RS-122-2001 TruSeq RNA Sample Prep Kit v2 (Illumina) as described in the manufacturer's instructions except for the final PCR step, for which eight PCR cycles were used. We used n=3 biological replicates for TCKD, n=4 biological replicates for TCKD-*Grhl2*KO, and n=5 biological replicates for control mice. Samples were pooled and sequenced on a NextSeq 500 device to generate 2×76 paired-end reads. Reads were demultiplexed and adapter-trimmed using flexbar[14] and mapped to the mm10 version of the mouse genome using tophat2; see Supplemental Figure 1 for re-analysis by using hisat2.[15] Sequencing reads per gene as annotated in the gencode mouse version M7 were counted using quasR,[16] and differential expression values calculated using edge.[17] Genes with a P value < 0.0001 for at least one

Table 3. Analyzed 5-week-old mice data from the indicated genotypes

ID	Sex	Age, wk	Mutation	Kidney Phenotype	BW, g	LKW, mg	RKW, mg	2KWs/BW, mg/g	BUN, mg/dl	Creatinine, mg/dl
KSX-07691	M	4.4	HoxB7/Cre+; R26StopFLMYC; Grhl2$^{flox/flox}$	Multiple cysts	8.1	264	238	62.0	128.85	0.40
KSX-07692	M	4.4	HoxB7/Cre+; R26StopFLMYC; Grhl2$^{flox/flox}$	Multiple cysts	7.4	368	370	99.7	137.25	0.43
KSX-06766	M	5.4	HoxB7/Cre+; R26StopFLMYC; Grhl2$^{flox/flox}$	Multiple cysts	8.7	294	301	68.4	101.12	0.34
KSX-07259	M	4.7	HoxB7/Cre+; R26StopFLMYC; Grhl2$^{flox/flox}$	Multiple cysts	7.5	318	332	86.7	137.25	0.43
KSX-07261	F	4.7	HoxB7/Cre+; R26StopFLMYC; Grhl2$^{flox/flox}$	Multiple cysts	5.5	223	220	80.5	122.13	0.40
KSX-07262	F	4.7	HoxB7/Cre+; R26StopFLMYC; Grhl2$^{flox/flox}$	Multiple cysts	4.9	135	141	56.3	145.66	0.44
KSX-07263	F	4.7	HoxB7/Cre+; R26StopFLMYC; Grhl2$^{flox/flox}$	Multiple cysts	9.8	375	390	78.1	137.25	0.29
KSX-07124	M	4.9	HoxB7/Cre+; R26StopFLMYC; Grhl2$^{flox/flox}$	Multiple cysts	6.8	180	225.5	59.6	77.31	0.27
KSX-07249	F	4.7	HoxB7/Cre+; R26StopFLMYC; Grhl2$^{flox/flox}$	Multiple cysts	7.2	250	233	67.1	140.06	0.37
KSX-07086	F	4.9	HoxB7/Cre+; R26StopFLMYC; Grhl2$^{flox/+}$	A few cysts	9.14	98	100	21.7	44.82	0.21
KSX-06956	F	5.3	HoxB7/Cre+; R26StopFLMYC; Grhl2$^{flox/+}$	A few cysts	11.7	113	129	20.8	27.73	0.19
KSX-06957	F	5.3	HoxB7/Cre+; R26StopFLMYC; Grhl2$^{flox/+}$	A few cysts	13.0	114	126	18.5	26.05	0.19
KSX-07693	M	4.4	HoxB7/Cre+; R26StopFLMYC; Grhl2$^{flox/+}$	A few cysts	9.64	97	98	20.2	30.81	0.23
KSX-07690	M	4.4	HoxB7/Cre+; R26StopFLMYC; Grhl2$^{flox/+}$	A few cysts	9.42	105	108	22.6	33.89	0.20
KSX-07698	F	4.4	HoxB7/Cre+; R26StopFLMYC; Grhl2$^{flox/+}$	A few cysts	8.28	68	73	17.0	39.22	0.20
KSX-07212	M	5.6	HoxB7/Cre+; R26StopFLMYC; Grhl2$^{flox/+}$	A few cysts	14.3	111	126	16.6	36.97	0.19
KSX-07080	M	4.9	HoxB7/Cre+; R26StopFLMYC; Grhl2$^{flox/+}$	A few cysts	12.5	96	104	16.0	30.81	0.19
KSX-07260	F	4.7	HoxB7/Cre+; R26StopFLMYC; Grhl2$^{flox/+}$	A few cysts	7	74	80	22.0	42.02	0.20
KSX-07700	F	4.4	R26StopFLMYC; Grhl2$^{flox/flox}$	Normal	10.9	57	58	10.6	25.77	0.19
KSX-07082	F	4.9	R26StopFLMYC; Grhl2$^{flox/flox}$	Normal	16.72	96	100	11.7	24.09	0.19
KSX-07083	F	4.9	R26StopFLMYC; Grhl2$^{flox/flox}$	Normal	13.9	87	92	12.9	26.61	0.19
KSX-06768	M	5.4	R26StopFLMYC; Grhl2$^{flox/flox}$	Normal	16.8	102	109	12.6	25.77	0.19
KSX-07250	F	4.7	R26StopFLMYC; Grhl2$^{flox/flox}$	Normal	16.6	102	103	12.3	24.37	0.19
KSX-07264	F	4.7	R26StopFLMYC; Grhl2$^{flox/flox}$	Normal	13.5	72	79	11.2	26.89	0.19
KSX-07085	F	4.9	R26StopFLMYC; Grhl2$^{flox/flox}$	Normal	14.37	85	91	12.2	26.61	0.19
KSX-06953	M	5.3	R26StopFLMYC; Grhl2$^{flox/flox}$	Normal	16.7	108	122	13.8	18.77	0.19
KSX-06954	M	5.3	R26StopFLMYC; Grhl2$^{flox/flox}$	Normal	19.1	127	135	13.7	17.93	0.19

HoxB7-Cre; R26StopFLMYC; Grhl2$^{flox/flox}$ referred as transgenic cystic kidney disease-*Grhl2* knockout, HoxB7-Cre; R26StopFLMYC; Grhl2$^{flox/+}$ referred as transgenic cystic kidney disease, and R26StopFLMYC; Grhl2$^{flox/flox}$ referred as control. BW, body weight; F, female; ID, mouse identification number; LKW, left kidney weight; M, male; RKW, right kidney weight.

of the three comparisons (TCKD-*Grhl2*KO versus TCKD, TCKD-*Grhl2*KO versus control, and TCKD versus control) were depicted as shown in the results. Raw data are available at the National Center for Biotechnology Information Gene Expression Omnibus database under the identifier GSE210217.

Statistical Analysis

Statistical analysis of each experiment is indicated in the result section. Data are presented as mean±SD. Tests were performed using the GraphPad Prism software, version 7.04. In brief, the Mann–Whitney *U* test was used for scoring intensity and fluorescence intensity analyses. For pairwise comparisons, the *t* test, and for multiple comparisons between different groups, one-way ANOVA followed by Tukey post-tests were used. P value < 0.05 was considered to be statistically significant.

Results

Reduced GRHL2 Protein Expression in Collecting Duct–Derived Cysts in Patients with ADPKD

We obtained kidney tissue samples from patients with ADPKD ($N=6$) and compared them with kidneys from patients without overt kidney disease referred as normal human kidneys ($N=4$). Clinical characteristics of patients with ADPKD are provided in Table 1. We applied immunofluorescence staining for GRHL2 protein and found it to be expressed within the principal and intercalated cells in the collecting duct of normal human kidneys. Specimens from patients with ADPKD are necessarily morphologically distorted. Because cyst generation in ADPKD occurs in various nephron portions,[18] we focused on GRHL2 expression pattern on collecting duct–derived cysts, which we labeled using the principal cell marker aquaporin-2 and the intercalated cell marker V-ATPase B1/2. We observed that collecting duct cells in kidneys from patients with ADPKD exhibited a significantly reduced GRHL2 expression, as detected by immunofluorescence staining for GRHL2 (magenta), aquaporin-2 (green), and V-ATPase B1/2 (red) (Figure 1). In normal collecting ducts from healthy human kidney tissue (Figure 1A), intercalated cells were found to be interspersed among principal cells. Compared with normal collecting ducts, the expression patterns of these markers in cyst-lining epithelia from patients with ADPKD were differently distributed. Some cysts were only positive for either the principal cell marker, aquaporin-2, or the intercalated cell marker, V-ATPase B1/2, while some cysts were positive for both markers (Figure 1, B and C). In samples of patients with ADPKD, kidney cysts that were derived from collecting ducts were determined by positive signals from either one

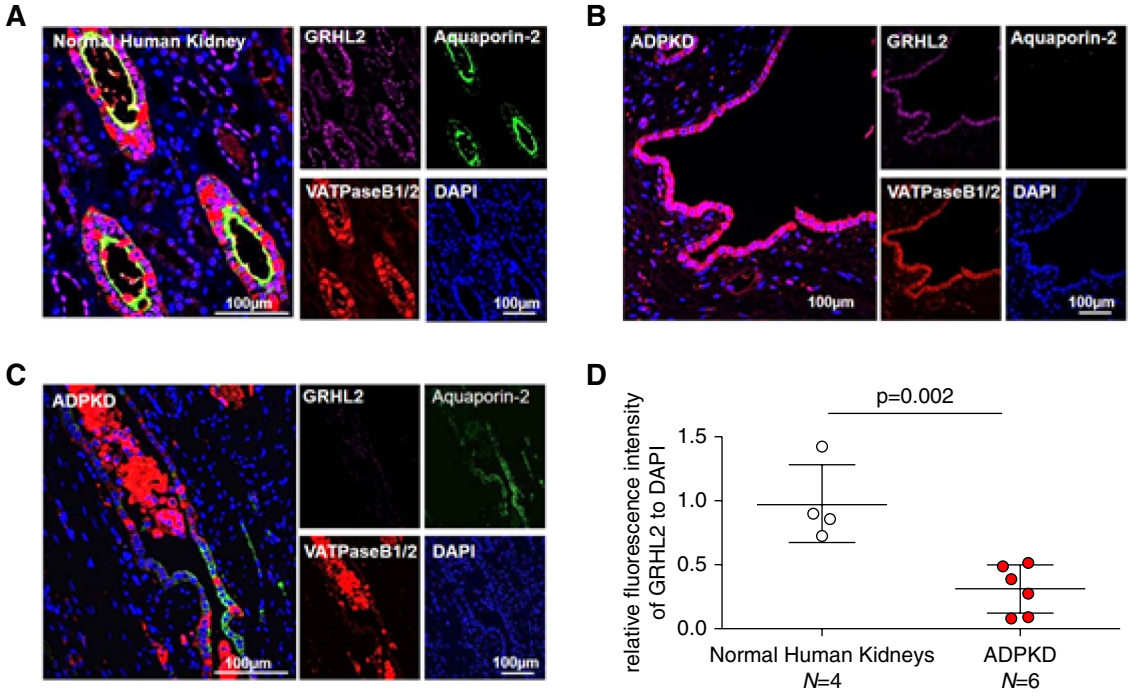

Figure 1. Analysis of GRHL2 protein expression in collecting duct–derived cysts in samples of patients with ADPKD. (A–C) Immunofluorescence staining on samples from normal human kidneys and patients with ADPKD was performed for GRHL2 (magenta) together with collecting duct cell markers, aquaporin-2 (green) and V-ATPase B1/2 (red), for principal and intercalated cells, respectively. Nuclei were stained with DAPI (blue). In normal human kidneys, intercalated cells were interspersed among principal cells of the normal collecting duct (A). In samples of patients with ADPKD, kidney cysts originating from collecting ducts were identified by the positivity of either aquaporin-2 or V-ATPase B1/2 or both of them. Representative images of GRHL2 positive (B) and negative (C) collecting duct–derived cysts are shown. (D) Quantitative analysis of GRHL2 fluorescence intensity within collecting duct cells on samples from normal human kidneys ($N=4$) and patients with ADPKD ($N=6$). GRHL2 fluorescence intensity was normalized to the fluorescence intensity of DAPI. Data are shown as mean±SD; P value was calculated with the Mann–Whitney *U* test. ADPKD, autosomal dominant polycystic kidney disease; DAPI, 4′,6-diamidino-2-phenylindole.

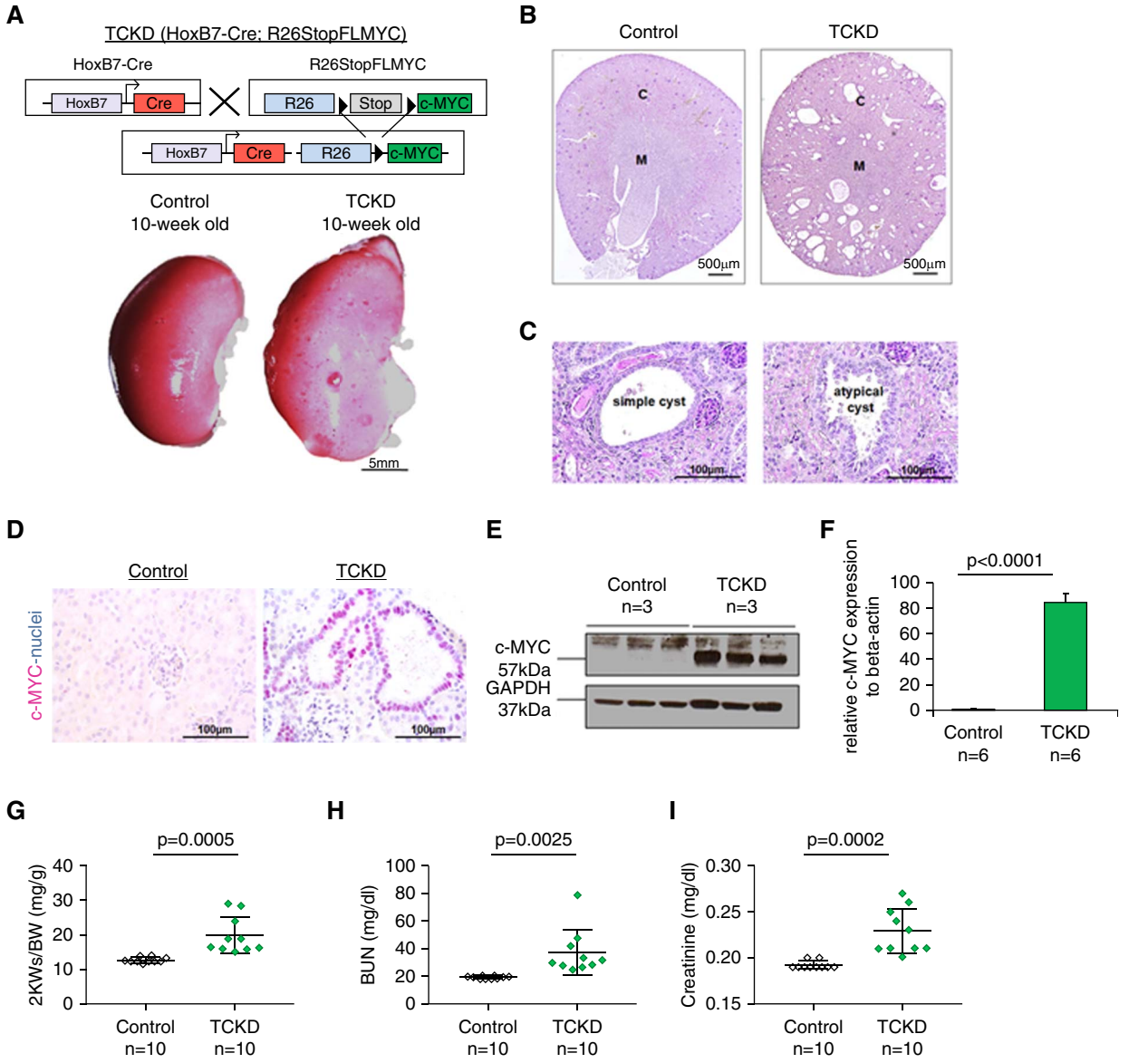

Figure 2. A novel model of TCKD. (A–C) Collecting duct–specific overexpression of the human proto-oncogene *c-MYC* in mice causes bilateral polycystic kidneys by 10 weeks of age. The breeding strategy of TCKD mice and gross kidney images from littermate controls and TCKD mice at 10 weeks of age (A). Comparative histological analysis of kidneys from control and TCKD mice, representative PAS-stained cross-kidney sections (B), and histological spectrum of simple and atypical cysts in kidneys of TCKD mice (C) are shown. (D) Immunohistochemical staining for c-MYC on kidneys from control and TCKD mice. There was no c-MYC–positive cell in the kidneys of control mice. Nuclei were stained with hematoxylin (blue). (E) Western blot analysis for c-MYC protein expression on total lysates from kidneys of control (n=3) and TCKD (n=3). There was no c-MYC protein expression in the kidneys of control mice compared with TCKD mice. GAPDH was used as a loading control. (F) RT-qPCR analysis for *c-MYC* expression was performed on lysates of whole kidneys from control (n=6) and TCKD mice (n=6). β-actin mRNA was used as an internal control. Data are shown as mean±SD. *P* values were calculated with the *t* test. (G–I) Graphs show the ratio of two KW over BW (G), BUN (H), and creatinine (I) measurements for 10-week-old control (n=10) and TCKD (n=10) mice. Data are mean±SD; *P* values were calculated with the *t* test. BW, body weight; C, cortex; GAPDH, glyceraldehyde 3-phosphate dehydrogenase; KW, kidney weight; M, medulla; PAS, periodic acid–Schiff; RT-qPCR, real-time quantitative PCR; TCKD, transgenic cystic kidney disease.

of these markers. GRHL2 expression was strongly present in the normal kidney collecting ducts (Figure 1A). By contrast, in collecting duct–derived cysts, GRHL2 protein expression was reduced or completely absent (Figure 1, B and C). To quantitate GRHL2 expression (Figure 1D), we analyzed fluorescence staining intensity. Cystic epithelia displayed a higher cell number per tubular cross-section compared with normal collecting duct epithelia. To control for this uneven distribution of collecting duct cells, we normalized the extracted staining intensity of GRHL2 for the staining intensity of 4′,6-diamidino-2-phenylindole (DAPI) within collecting duct cells. Quantitative analysis of GRHL2 fluorescence intensity revealed a 65% reduction in collecting duct–derived cysts in patients with

ADPKD compared with its fluorescence intensity in collecting ducts of normal human kidneys. These data indicated that GRHL2 protein expression is reduced in collecting duct–derived cysts from patients with ADPKD.

c-MYC Overexpression in the Collecting Duct Results in Cystic Kidney Disease

We next generated a TCKD mouse model involving the overexpression of the human proto-oncogene *c-MYC* in renal collecting ducts to produce a model of cystic kidney disease with exclusively collecting duct–derived cysts (Figure 2). *c-MYC* is overexpressed in cyst-lining epithelia of patients with PKD,[19,20] and its overexpression in tubular epithelial cells in mice has previously been reported to result in PKD.[21,22] We used HoxB7-Cre mice that direct Cre recombinase into collecting duct epithelia and crossed them with R26StopFLMYC mice, which overexpress the human *c-MYC* in response to Cre-mediated recombination in the ROSA26 locus.[13] The resulting HoxB7-Cre; R26StopFLMYC mice activated expression of *c-MYC* exclusively in collecting duct cells (Figure 2A). To avoid nomenclature confusion, we subsequently refer to HoxB7-Cre; R26StopFLMYC mice simply as TCKD mice.

We found that TCKD mice developed grossly abnormal kidneys at 10 weeks of age, which included overt cystic lesions within collecting duct cells. Histological analysis of kidneys from 10-week-old TCKD mice revealed that the cysts were exclusively confined to the cortex and the outer medulla (Figure 2B). The cysts ranged from simple cysts (single layer of cells lined around a lumen) to atypical cysts (cysts lined by two or three layers of cells) (Figure 2C). As expected from the design of this mouse model, there was no detectable change in proximal tubules and glomeruli because these cells do not express Cre and, therefore, do not overexpress *c-MYC*. The expression of human *c-MYC* was detectable only in the kidneys of TCKD mice but not in the kidneys of littermate controls, as shown by immunohistochemical staining for c-MYC and Western blot analysis as well as RT-qPCR (Figure 2, D–F, and see Supplemental Figures 2A and 3A). These results indicate that the cysts are a direct consequence of the collecting duct–specific overexpression of the human proto-oncogene *c-MYC*. The ratio of the weight of both kidneys over body weight was markedly and significantly increased in TCKD mice compared with controls (Figure 2G and Table 2). BUN and creatinine levels were increased in TCKD mice, indicating impaired kidney function (Figure 2, H and I, and Table 2). Eventually, kidney failure ensued by 12 weeks of age.

TCKD Mice Display Hyperproliferation of Principal and Intercalated Cells

We next attempted to determine the cellular mechanisms of cyst formation in TCKD mice (Figure 3). For this purpose, we performed immunofluorescence staining with collecting duct cell markers, aquaporin-2 (green) and V-ATPase B1/2 (red), for principal and intercalated cells, respectively, on kidneys from TCKD and littermate controls at 10 weeks of age. In control kidneys, intercalated cells were interspersed among the principal cells in collecting ducts. In TCKD mice, we found that clusters of intercalated and principal cells developed, disrupting the normal architecture of these cells (Figure 3A). This was particularly pronounced in collecting ducts from the cortex and the outer medulla, which displayed cyst formation, but much less pronounced in collecting ducts of the inner medulla, which did not display cyst formation.

We hypothesized that *c-MYC* overexpression might result in abnormal cell proliferation with subsequent cyst formation in TCKD mice. We therefore performed immunofluorescence staining for the proliferation marker, Ki67 (white), combined with collecting duct cell markers aquaporin-2 and V-ATPase B1/2 using kidneys from TCKD and littermate controls at 10 weeks of age (Figure 3B). Quantitative analysis revealed marked and significant increases in the percentage of Ki67-positive aquaporin-2 and Ki67-positive V-ATPase B1/2 in the cortex and the outer medulla of kidneys from TCKD mice compared with control mice (Figure 3, C and D). By contrast, there were only mild or absent changes in the numbers of collecting duct cells in the inner medulla. Hence, *c-MYC* overexpression resulted in strongly increased proliferation of principal and intercalated cells in TCKD mice.

We next investigated Grhl2 protein expression in TCKD mice at 10 weeks of age with immunohistochemistry (Figure 3E). In TCKD mice, cyst-lining cells were uniformly positive for Grhl2 staining. In control mice, the expression of Grhl2 was restricted in the cells of distal tubules and collecting ducts, consistent with the known expression pattern of Grhl2 in mouse kidney.[9] Grhl2 protein and mRNA levels were significantly increased in extracts from TCKD kidneys compared with control kidneys (Figure 3, F and G, and see Supplemental Figure 2B). These observations were consistent with an increased abundance of Grhl2-positive principal and intercalated cells in TCKD kidneys.

Grhl2 Deletion Strongly Aggravates the Disease Progression in the TCKD Model

To test the underlying hypothesis that Grhl2 may modify the course of cystic kidney disease, we conditionally inactivated *Grhl2* in collecting ducts of TCKD mice (Figure 4). We purposely focused on the collecting ducts because of the expression pattern of Grhl2 in the kidney. The collecting duct–specific deletion of *Grhl2* in healthy kidneys in mice has been published.[10] We bred TCKD mice with mice harboring a floxed *Grhl2* allele.[8] This resulted in mice carrying HoxB7-Cre; R26StopFLMYC; $Grhl2^{flox/flox}$ genotype, allowing simultaneous HoxB7-Cre–mediated homozygous deletion of *Grhl2* and overexpression of *c-MYC* in collecting duct cells. We refer to these mice as TCKD-*Grhl2*KO. At 5 weeks of age, TCKD-*Grhl2*KO mice had massively enlarged kidneys compared with TCKD mice (Figure 4A). Cysts were not only present in the cortex but also in the medulla. The influence of absent *Grhl2* was dramatic compared with TCKD mice (Figure 4, C and D). At this age, there were slight changes in the kidneys of TCKD mice compared with control kidneys; only a few cysts were visible in the cortex (Figure 4, B and C, dashed box, arrowheads).

To determine the age onset of cyst initiation, we examined TCKD and TCKD-*Grhl2*KO kidneys at different ages including postnatal day (P) 1 and P18 compared with control mice (Figure 4, E–G). Comparative histological analysis starting at P1 revealed that the absence of *Grhl2*

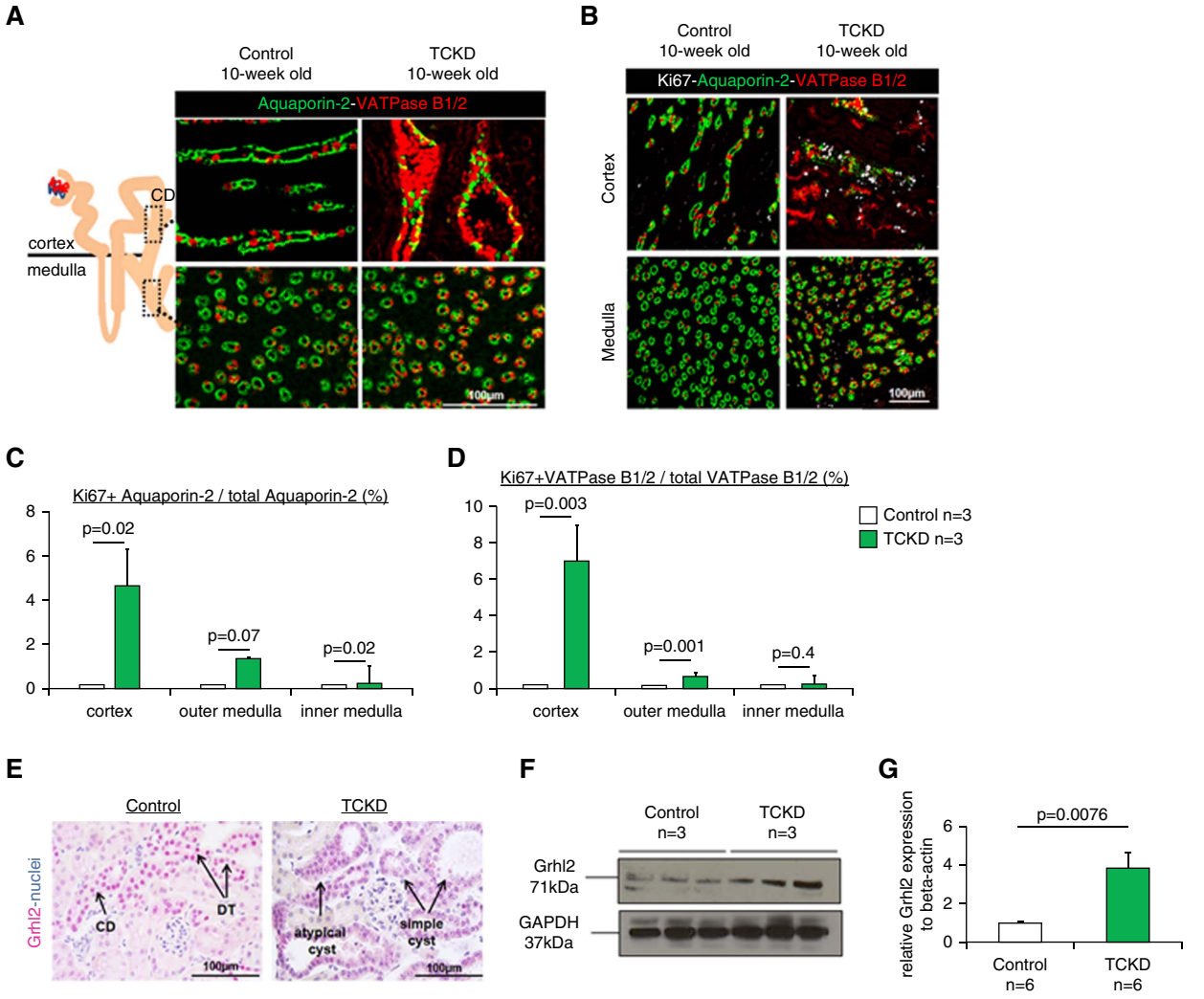

Figure 3. Expression patterns of collecting duct cell markers and Grhl2 in cyst-lining epithelia in TCKD mice. (A) Characterization of the cellular origin of cysts was investigated with immunofluorescence staining of collecting duct cells markers, aquaporin-2 (green) and V-ATPase B1/2 (red), for principal and intercalated cells, respectively, on kidneys from control and TCKD mice at 10 weeks of age. (B) Immunofluorescence staining for the proliferation marker, Ki67 (white), combined with collecting duct cell markers, aquaporin-2 and V-ATPase B1/2, were performed on kidneys from control and TCKD mice at 10 weeks of age to quantify the proliferation rate of collecting duct cells. Representative images are shown from the cortex and the medulla of kidneys from each indicated genotype. (C and D) Graphs show the percentage of Ki67-positive aquaporin-2 and Ki67-positive V-ATPase B1/2 cells regarding three main regions of kidneys from control and TCKD mice. Data are shown as mean±SD; *P* values were calculated with the *t* test. (E–G) TCKD mice expressed Grhl2 to a greater degree than control mice as shown both at the protein and mRNA levels. (E) Immunohistochemical staining for Grhl2 on kidneys from control and TCKD mice at 10 weeks of age. Nuclei were stained with hematoxylin (blue). (F) Western blot analysis for Grhl2 protein expression on total lysates from kidneys of control ($n=3$) and TCKD ($n=3$). GAPDH was used as a loading control. (G) RT-qPCR analysis for *Grhl2* expression was performed on lysates of whole kidneys from control ($n=6$) and TCKD mice ($n=6$). β-actin mRNA was used as an internal control. Data are mean±SD; *P* values were calculated with the *t* test. CD, collecting duct; DT, distal tubule.

resulted in dilated collecting duct tubules (Figure 4G, see P1, black arrow) and cysts in the medulla (Figure 4G, see P1, arrowheads). At P18, the cysts began to cover the entire TCKD-*Grhl2*KO kidney (Figure 4G, see P18), whereas there were only rare isolated cysts in TCKD mice (Figure 4F, see P18, arrowhead). These findings demonstrate that cyst initiation occurred during embryonic development and expanded rapidly and progressively in the kidneys of TCKD-*Grhl2*KO mice, resulting in significantly enlarged kidneys. TCKD-*Grhl2*KO mice developed increased kidney weights to body weight ratio (Figure 4H and Table 3) and increased levels of BUN and creatinine (Figure 4, I and J, and Table 3), indicating that these mice had kidney failure at early ages (4–6 weeks). Thus, collecting duct–specific deletion of *Grhl2* in kidneys of TCKD mice aggravated cyst growth, worsened kidney dysfunction, and shortened life span. These findings demonstrate that the presence of Grhl2 in collecting duct epithelia is necessary to prevent excessive cyst development in our model.

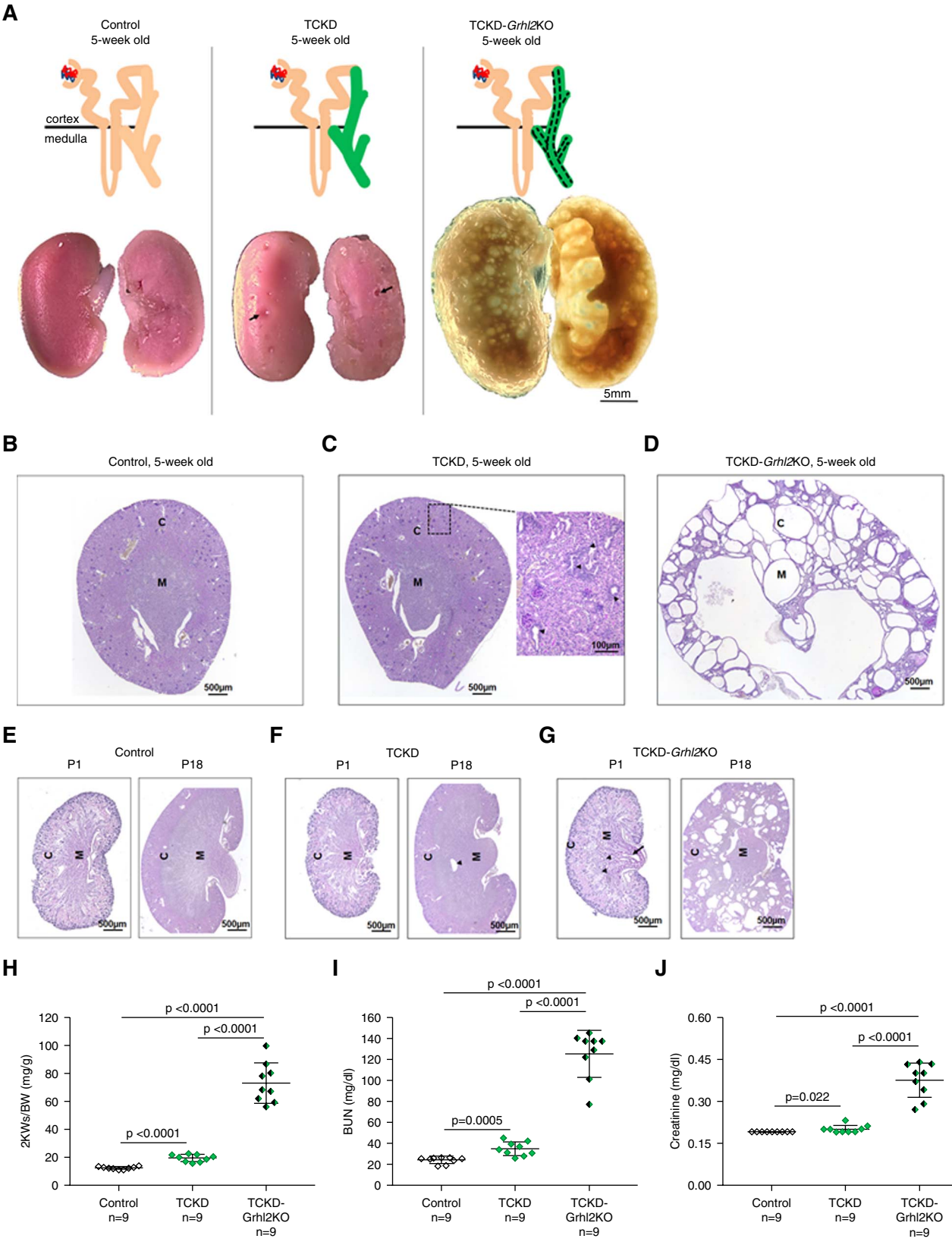

Figure 4. A cross of TCKD and a collecting duct *Grhl2*-deleted model reveals rampant cyst development. (A) Schematic representation of the genetic modifications of the generated mouse models and gross images of kidneys from the indicated genotypes at 5 weeks of age. Representative bisected kidney images from the outsides and insides of control, TCKD, and TCKD-*Grhl2*KO mice. While there are a few cystic lesions (black arrows) on the kidney of TCKD mice, the kidney architecture was almost entirely demolished in TCKD-*Grhl2*KO mice.

Figure 4. *Continued.* (B–G) Comparative histological analysis of kidneys from control, TCKD, and TCKD-*Grhl2*KO mice at different ages, *i.e.*, representative PAS-stained kidney sections from postnatal day 1 (P1), P18, and 5 weeks. Compared with control mice, there was no dramatic change in the kidneys of TCKD mice at P1 and P18 (E and F), whereas cystic abnormalities became visible at 5 weeks of age (dashed box, arrowheads at higher magnifications) (B and C). At 5 weeks of age, massively enlarged kidney of TCKD-*Grhl2*KO mice due to cyst formation (D). At P1, collecting duct tubular dilation (black arrow) and small cysts (arrowheads) were already visible in TCKD-*Grhl2*KO mice. At P18, the kidneys of TCKD-*Grhl2*KO mice were almost completely covered by cysts of various sizes (G). Graphs show the two KW over BW ratios (H), BUN (I), creatinine (J) measurements for 5-week-old control (n=9), TCKD (n=9), and TCKD-*Grhl2*KO (n=9) mice. Data are mean±SD; P values were calculated with one-way ANOVA, Tukey's multiple comparison tests. *Grhl2*KO, *Grhl2* knockout.

Grhl2 Acts as a Gatekeeper of Unregulated Cell Proliferation

To confirm the loss of Grhl2 expression in the kidneys of TCKD-*Grhl2*KO mice, we performed RT-qPCR and Western blot analysis (Figure 5, A and B, and see Supplemental Figure 2C). Consistent with histological examinations, we determined that the expression of Grhl2 was significantly reduced at both the mRNA and protein levels in kidneys of TCKD-*Grhl2*KO mice compared with their littermate controls at 5 weeks of age. RT-qPCR analysis revealed an eight-fold decrease in the expression of *Grhl2* in the kidneys of TCKD-*Grhl2*KO mice compared with TCKD mice. Similarly, Grhl2 protein expression was remarkably reduced in the kidneys of TCKD-*Grhl2*KO mice compared with TCKD mice. Notably, because of incompletely efficient HoxB7-Cre activity,[10] residual expression of Grhl2 was still detectable in the kidneys of TCKD-*Grhl2*KO mice (Figure 5A).

To test whether *c-MYC* overexpression changes because of *Grhl2* deletion, we performed RT-qPCR and Western blot analysis from kidneys of 5-week-old TCKD-*Grhl2*KO, TCKD, and control mice (Figure 5, C and D, and see Supplemental Figure 2D). RT-qPCR analysis revealed overexpression of *c-MYC* in kidneys of TCKD mice compared with control mice, and its overexpression further increased by 1.6-fold in kidneys of TCKD-*Grhl2*KO mice compared with TCKD. Similarly, at the protein level, an increased c-MYC overexpression was determined using Western blot analysis. Collectively, the increase in *c-MYC* expression in TCKD-*Grhl2*KO mice is most like secondary to the excessive expansion of collecting duct–derived cysts.

c-MYC gene is known to regulate proliferation and apoptosis in the course of PKD.[19,20] As demonstrated in Figure 3, B–D, *c-MYC* overexpression increased cell proliferation in the kidneys of TCKD mice. Based on this finding, to test whether *Grhl2* deletion promotes proliferation, we examined cell proliferation in collecting ducts from 5-week-old TCKD-*Grhl2*KO mice (n=3) compared with their littermate controls (n=3 each) (Figure 5, E–G). Immunofluorescence staining for Ki67 (white) and collecting duct cell markers revealed that *Grhl2* deletion potentiated collecting duct cells' proliferation dramatically in the entire kidney (Figure 5E). Specifically, the quantification of Ki67-positive aquaporin-2 cells revealed a 2.3-fold increase in the cortex and a 3.5- to 9-fold increase in the outer and inner medulla, respectively (Figure 5F). Similarly, Ki67-positive VATPase B1/2 cells increased 1.2-fold in the cortex and 4.8- to 7.5-fold in the outer and the inner medulla, respectively (Figure 5G). Although the abnormal proliferation of collecting duct cells led to cyst formation in kidneys of both transgenic mouse models, *Grhl2* deletion potentiated proliferation, resulting in cyst aggravation. Taken together, these findings indicate that Grhl2 acts as a gatekeeper of uncontrolled cell proliferation in the generated TCKD model.

To test whether the dysregulation of cellular proliferation was associated with apoptosis, we performed immunohistochemical staining for cleaved caspase 3 on kidneys from P1, P18, and 5-week-old TCKD-*Grhl2*KO, TCKD, and control mice. Analysis of P1 mice kidneys revealed a high number of cleaved caspase 3 positive cells in the kidneys of TCKD-*Grhl2*KO mice compared with TCKD mice and control mice (Figure 5H). Detailed analysis of cleaved caspase 3–positive cells showed that there was a significant increase in the number of apoptotic cells in the kidneys of P1 and P18 mice but not in the adult mice kidneys (the data from P18 and 5-week-old mice were not shown). Thus, *Grhl2* deletion noticeably upregulates apoptosis that might be related to tubular dilation in the setting of cyst formation.

Grhl2 Acts as a Modifier of Collecting Duct–Derived Cyst Formation

To elucidate the genetic mechanisms in the massively enlarged polycystic kidney phenotype of TCKD-*Grhl2*KO mice and to address the target genes of Grhl2 in the context of cystic kidney disease, we performed RNA-seq analysis. To avoid analyzing secondarily affected genes due to disease progression, we performed this experiment at the precystic stage. Total RNAs were extracted at P1 from entire TCKD-*Grhl2*KO kidneys (n=4), TCKD (n=3), and control mice (n=5) (Figure 6, A–C).

RNA-seq data analysis revealed the differentially expressed gene profiles between the kidneys of TCKD-*Grhl2*KO, TCKD, and control mice. Consistent with histological examinations, the most affected genes were the result of *Grhl2* deletion (Figure 6, A–C). As demonstrated in Figure 4, E and F, at P1, there was no dramatic histological change between the kidneys of TCKD mice and control mice. Similarly, the RNA-seq analysis revealed only three genes—Keratin 14 (*Krt14*), the forkhead transcription factor, Forkhead boxi1 (*Foxi1*), and small nucleolar RNA host gene 4 (*Snhg4*)—with a >2-fold overexpression (false discovery rate <0.01 and P values < 0.0001) in kidneys of TCKD mice compared with control mice at P1 (Figure 6C). However, comparison of gene expression profiles between the kidneys of TCKD-*Grhl2*KO mice and TCKD mice revealed that 51 genes were >2-fold differentially expressed (false discovery rate <0.01 and P values < 0.0001) on *Grhl2* deletion. Seventeen were upregulated and 34 were downregulated in TCKD-*Grhl2*KO kidneys (Figure 6A and Table 4).

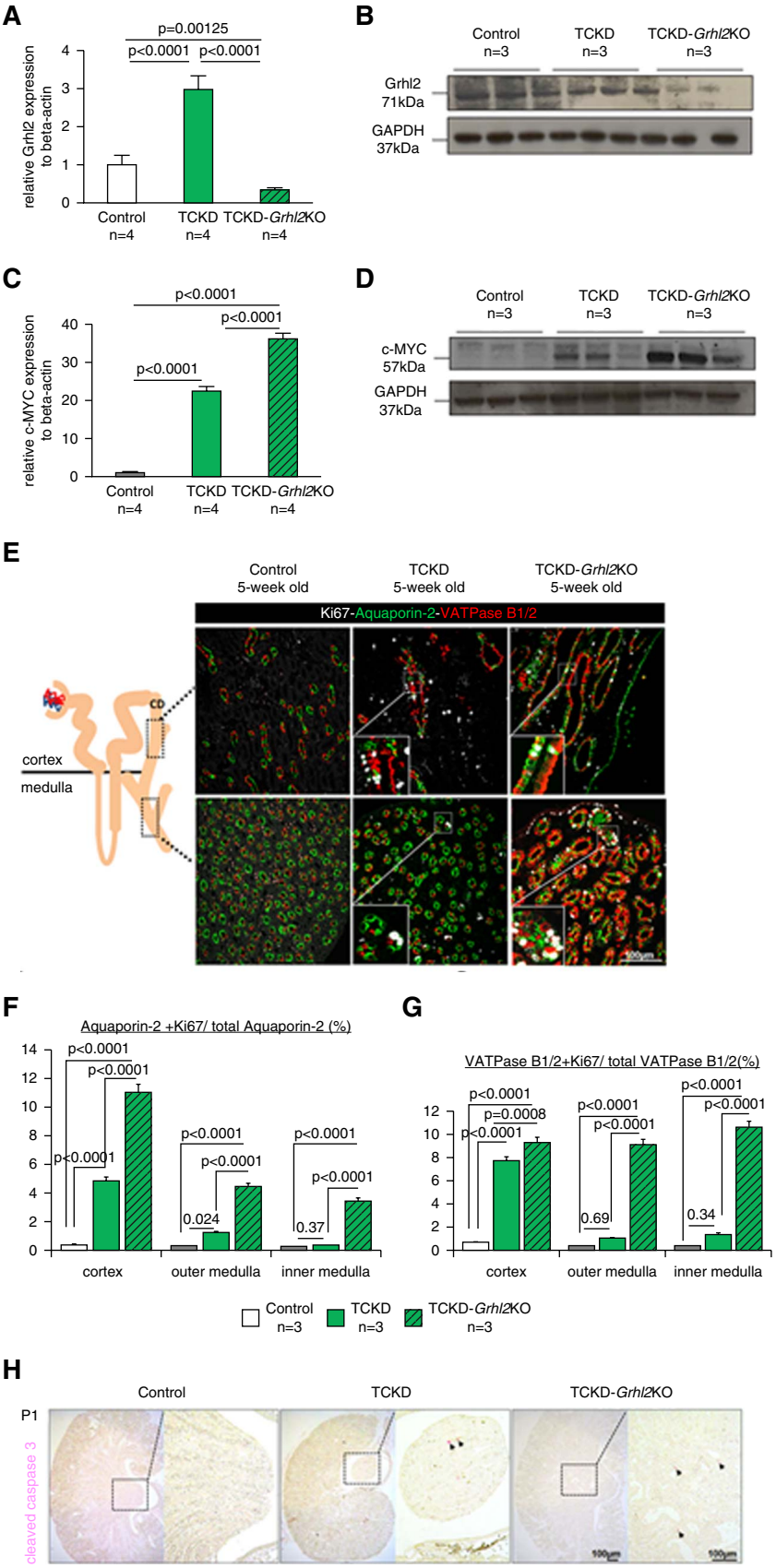

Figure 5. *Grhl2* deletion in TCKD mice promotes collecting duct cell proliferation and apoptosis. (A and C) RT-qPCR analyses show the expressions of *Grhl2* (A) and c-*MYC* (C) in kidneys from control, TCKD, and TCKD-*Grhl2*KO mice (n=4 for each mice) at 5 weeks of age.

Figure 5. *Continued.* β-actin mRNA was used as an internal control. Data are shown as mean±SD. *P* values were calculated with one-way ANOVA, Tukey's multiple comparisons tests. (B and D) Western blot analyses show Grhl2 (B) and c-MYC (D) protein abundance in kidney lysates from 5-week-old control and transgenic mice ($n=3$ for each mice). GAPDH was used as a loading control. While Grhl2 expression was decreased, c-MYC overexpression was increased at both the mRNA and protein levels in the kidneys of TCKD-*Grhl2*KO mice compared with TCKD mice. (E) Immunofluorescence staining for the proliferation marker, Ki67 (white), combined with collecting duct cell markers, aquaporin-2 (green) and V-ATPase B1/2 (red), were performed on kidneys from control, TCKD, and TCKD-*Grhl2*KO mice at 5 weeks of age. Representative images are shown from the cortex and the medulla of kidneys from the indicated genotypes. (F and G) Graphs show the percentage of Ki67-positive aquaporin-2 cells (F) and Ki67-positive V-ATPaseB1/2 cells (G) regarding three main regions of kidneys from control, TCKD, and TCKD-*Grhl2*KO mice. Data are shown as mean±SD; *P* values were calculated with the *t* test. (H) Immunohistochemical staining of cleaved caspase 3 was performed on kidneys from each indicated genotype at P1. At higher magnification, arrowheads in the kidneys of TCKD-*Grhl2*KO and TCKD mice show cleaved caspase 3 positive (pink) cells.

Gene ontology analysis of differentially expressed genes using the Database for Annotation, Visualization, and Integrated Discovery software[23,24] indicated enrichment in proliferation, programmed cell death, cell-cell adhesion, epithelial cell differentiation, ureteric bud development, and water homeostasis (Figure 6D).

Moreover, we used our previously published Grhl2 chromatin immunoprecipitation-seq data that were performed on kidneys from E18 mice[9] to analyze the potential association of Grhl2 with regulatory regions of these differentially expressed genes. We found that 20 genes (asterisks in Figure 6A), *i.e.*, one upregulated gene (5.9%) and 19 downregulated genes (55.9%), had Grhl2-binding sites (chi-square statistics 10.0738, significant at $P < 0.01$), indicating that a large proportion of the downregulated genes might be directly regulated by Grhl2. To further validate the differentially expressed genes obtained by RNA-seq, we performed RT-qPCR analysis for 12 randomly selected genes from kidneys of control, TCKD, and TCKD-*Grhl2*KO mice ($n=3$ for each) at P1, confirming the results of RNA-seq (Supplemental Figure 4).

Furthermore, based on published studies, we identified three genes, namely Fras1-related extracellular matrix protein 2 (*Frem2*),[25] Mucin1 (*Muc1*),[26] and cyclin-dependent kinase inhibitor 2c (*Cdkn2c*)[27] that are involved in either cyst initiation or progression, suggesting that these are candidate drivers of the phenotype. In addition, we used RT-qPCR to examine the expression profiles of cystic kidney disease–related genes, ADPKD genes *Pkd1* and *Pkd2*, the tuberous sclerosis complex gene *Tsc1*, and the RCAD syndrome gene Hnf1β in kidneys from control, TCKD, and TCKD-*Grhl2*KO mice at P1 and 5 weeks of age (Figure 6, E–H). At P1, there was no significant change in the expression levels of any of these genes between the kidneys of TCKD-*Grhl2*KO and TCKD mice compared with control mice, consistent with RNA-seq data. At 5 weeks, there was no significant change in *Pkd1* (Figure 6E) and Hnf1β expression (Figure 6H) between the kidneys of TCKD-*Grhl2*KO and TCKD mice as well as compared with control mice. However, *Pkd2* (Figure 6F) and *Tsc1* (Figure 6G) expression were significantly reduced in kidneys of TCKD-*Grhl2*KO compared with TCKD mice at 5 weeks. Hence, reduced expression of *Pkd2* and *Tsc1* during cystic kidney disease progression might further contribute to the progressive cyst development in TCKD-*Grhl2*KO mice.

Discussion

We made three key findings. First, transcription factor GRHL2 displayed downregulation in collecting duct–derived cyst in patients with ADPKD. Second, we developed a novel mouse model of collecting duct–derived cyst formation based on overexpression of *c-MYC* that resulted in slowly progressive cystic kidney disease. In this specific PKD model, deletion of *Grhl2* led to rampant collecting duct epithelial cell proliferation and cyst development, indicating that *Grhl2* may act as a gatekeeper of uncontrolled collecting duct proliferation. Third, in *Grhl2*-deficient TCKD mice, we found downregulation of several genes whose loss had been previously linked to cyst formation, suggesting that Grhl2 controls a gene program that preserves collecting duct epithelial integrity in the setting of a cyst-inducing stimulus. Our findings highlight the possibility that Grhl2 and its putative targets may act as a modifier of cystic kidney disease progression in collecting duct epithelia.

The clinical course of PKD is highly variable, suggesting an importance of modifier genes.[6,28] Our prediction of Grhl2 as a potential modifier of cystic kidney disease progression in human PKD on the basis of the results presented herein will require confirmation in future studies.

Modeling PKD is difficult.[29] The ultimate goal of a mouse model of disease is to genetically manipulate the disease gene in question and to derive a phenotype that closely mimics the human disease. The first genetically engineered mouse mutant of PKD1 was a targeted deletion of exon 34 in mouse *Pkd1* that resulted in perinatal death due to kidney cystic disease in homozygous mice. However, heterozygous mice developed multiple bilateral cortical and medullary kidney cysts by 16 months of age, as well as liver cysts derived from the biliary epithelium.[30] Different disruptions in *Pkd1* produced variable phenotypes.[31] Subsequent models focused on various levels of *Pkd1* expression. Conditional deletion approaches have also been applied.[32] Despite vast progress made in modeling PKD, the precise disease mechanisms remain elusive. None of these models perfectly recapitulate the complexity of the human disease.[33]

Trudel *et al.* first developed a transgenic PKD mouse model, SBM, by introducing into the genome a hybrid construct containing the SV40 enhancer, β-globin promoter, and *c-Myc* proto-oncogene.[21] They found that increased expression of *c-Myc* was correlated with the initiation

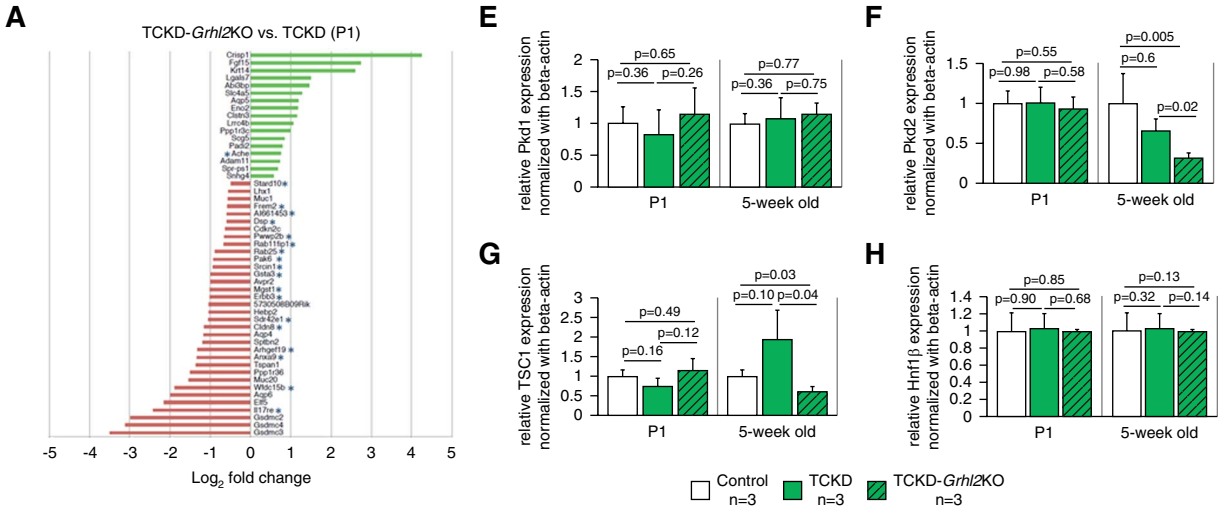

D

Gene Ontology Term	Genes
cell junction (cell-cell adhesion)	Ache, Erbb3, Frem2, Srcin1, Clstn3, Sptbn2, Pak6, Anxa9, Abi3bp, Cldn8, Dsp
epithelial cell differentiation	Muc1, Krt14, Rab25
programmed cell death and necrosis	Gsdmc2, Gsdmc3, Gsdmc4, Lgals7, Muc20, Hebp2
regulation of cell proliferation	Tspan1, Avpr2, Cdkn2c
ureteric bud development	Gsta3, Lhx1
water homeostasis	Aqp4, Aqp5, Aqp6

Figure 6. Identification of Grhl2 target genes in the context of cystic kidney disease. (A–C) RNA-seq analysis was performed on lysates of whole kidneys from control (n=5), TCKD (n=3), and TCKD-*Grhl2*KO (n=4) mice at P1. (A) Differentially expressed genes between the kidneys of TCKD-*Grhl2*KO mice and TCKD mice at P1. Genes upregulated in TCKD-*Grhl2*KO kidneys compared with TCKD kidneys are labeled in green; downregulated genes are labeled in red. Bars indicate $\log_2$-fold changes (FDR <0.01 and P values < 0.0001). Genes whose regulatory genomic regions had been previously identified to be bound by Grhl2 according to ChIP-seq from wild-type E18 mouse kidneys are labeled by asterisks. (B) Differentially expressed genes between the kidneys of TCKD-*Grhl2*KO mice compared with control mice at P1. (C) Differentially expressed genes between the kidneys of TCKD mice and control mice at P1. (D) GO analysis of differentially expressed genes between the kidneys of TCKD-*Grhl2*KO mice and TCKD mice. (E–H) RT-qPCR analyses show the expression of cystic kidney disease–related genes *Pkd1* (E), *Pkd2* (F), *Tsc1* (G), and *Hnf1β* (H) in kidneys from control, TCKD, and TCKD-*Grhl2*KO mice (n=3 each) at P1 and at 5 weeks. There was no significant change in the expression levels of any cystic kidney disease–related genes between the kidneys of TCKD-*Grhl2*KO and TCKD mice compared with control mice at P1. (E and H) There was no significant change in the expression levels of *Pkd1* (E) and *Hnf1β* (H) in the kidneys of TCKD-*Grhl2*KO and TCKD mice compared with control mice at 5 weeks. (F and G) At 5 weeks of age, *Pkd2* (F) and *Tsc1* (G) expression levels were significantly downregulated in the kidneys of TCKD-*Grhl2*KO mice compared with TCKD mice and control mice. There was no significant change in the expression levels of these genes in the kidneys of TCKD mice compared with control mice at 5 weeks. Data are shown as mean±SD. P values were calculated with the t test. ChIP, chromatin immunoprecipitation; FDR, false discovery rate; GO, gene ontology; RNA-seq, RNA-sequencing.

and progression of the PKD phenotype as evidenced by early tubular and glomerular cysts in SBM mouse kidneys. The cyst number and size increased with age, with codevelopment of glomerular and tubular epithelial hyperplasia. The investigators determined that the mean renal proliferative index was increased approximately 5- to 20-fold in noncystic and cystic tubules of newborn SBM animals compared with littermate controls.

Table 4. List of differentially expressed genes from RNA sequencing

Gene Symbol	Gene Description
Crisp1	Cysteine-rich secretory protein 1
Fgf15	Fibroblast growth factor 15
Krt14	Keratin 14
Lgals7	Lectin, galactose binding, soluble 7
Abi3bp	ABI gene family, member 3 (NESH) binding protein
Slc4a5	Solute carrier family 4, sodium bicarbonate cotransporter, member 5
Aqp5	Aquaporin 5
Eno2	Enolase 2, gamma neuronal
Clstn3	Calsyntenin 3
Lrrc4b	Leucine rich repeat containing 4B
Ppp1r3c	Protein phosphatase 1, regulatory (inhibitor) subunit 3C
Scg5	Secretogranin V
Padi2	Peptidyl arginine deiminase, type 2
Ache	Acetylcholinesterase
Adam11	A disintegrin and metallopeptidase domain 11
Spr-ps1	Sepiapterin reductase pseudogene 1
Snhg4	Small nucleolar RNA host gene 4
Stard10	START domain containing 10
Lhx1	LIM homeobox protein 1
Muc1	Mucin 1, transmembrane
Frem2	Fras1 related extracellular matrix protein 2
AI661453	AI661453
Dsp	Desmoplakin
Cdkn2c	Cyclin-dependent kinase inhibitor 2C (p18, inhibits CDK4)
Pwwp2b	PWWP domain containing 2B
Rab11fip1	RAB11 family interacting protein 1 (class I)
Rab25	RAB25, member RAS oncogene family
Pak6	p21 protein (Cdc42/Rac)-activated kinase 6
Srcin1	SRC kinase signaling inhibitor 1
Gsta3	Glutathione S-transferase, α 3
Avpr2	AVP receptor 2
Mgst1	Microsomal glutathione S-transferase 1
Erbb3	Erb-b2 receptor tyrosine kinase 3
5730508B09Rik	5730508B09Rik
Hebp2	Heme binding protein 2
Sdr42e1	Short chain dehydrogenase/reductase family 42E, member 1
Cldn8	Claudin 8
Aqp4	Aquaporin 4
Sptbn2	Spectrin β, non-erythrocytic 2
Arhgef19	Rho GEF 19
Anxa9	Annexin A9
Tspan1	Tetraspanin 1
Ppp1r36	Protein phosphatase 1, regulatory subunit 36
Muc20	Mucin 20
Wfdc15b	WAP four-disulfide core domain 15B
Aqp6	Aquaporin 6
Elf5	E74-like factor 5
Il17re	Interleukin 17 receptor E
Gsdmc2	Gasdermin C2
Gsdmc4	Gasdermin C4
Gsdmc3	Gasdermin C3

ABI, NESH (Abelson interactor protein 3); AVP, arginine vasopressin; GEF, guanine nucleotide exchange factor; LIM, a protein domain involved in protein–protein interactions; PWWP, proline-tryptophan-tryptophan-proline; RAS, renin-angiotensin system; SRC, tyrosine-protein kinase Src; START, steroidogenic acute regulatory protein-related lipid transfer domain.

As our study addressed a proof of principle, we embarked on establishing our PKD model restricted to cells of the kidney collecting duct. We were aware that the c-Myc oncogene plays a pivotal role in PKD[19–22] and therefore aimed to overexpress *c-MYC* in the collecting duct by generating TCKD mice. The phenotypic features of these mice resemble the slowly progressive development of cysts throughout life that is also observed in human PKD. These mice have particular utility for addressing our hypothesis of an involvement of Grhl2 in PKD because *Grhl2* expression is restricted to epithelia of the distal nephron and the collecting duct and absent in proximal tubular epithelia.

Our group previously identified a relationship between GRLH2 and osmoregulation. Collecting duct–specific deletion of *Grhl2* in mice led to reduced expression of tight junction–associated barrier components, reduced collecting duct transepithelial resistance, and defective renal medullary accumulation of sodium and other osmolytes.[10,34] The data indicated a direct functional link between collecting duct epithelial barrier

characteristics, which seem to prevent leakage of interstitial osmolytes into urine, and body water homeostasis. Interestingly, the sole therapeutic agent to convincingly alter the progression of ADPKD to date is tolvaptan, a blocker of the vasopressin V2 receptor, which is expressed in collecting duct epithelia.[12] This raises the possibility that GRHL2-mediated alternations of epithelial characteristics, including vasopressin responsiveness, might contribute to the phenotypes we observed here.

We observed that *Grhl2* deletion potentiates cell proliferation and cyst progression, which was associated with reduced expression of *Frem2*, encoding the Fras1-related extracellular matrix protein 2. This extracellular matrix protein, associated with Fraser Syndrome, is believed to be required for maintaining the integrity of the skin epithelium and the differentiated state of renal epithelia.[25] Another *Grhl2* target gene is *Muc1* encoding mucin 1. Additionally, Grhl2 may regulate the expression of the cyclin-dependent kinase inhibitor 2C, encoded by the Cdkn2 gene. All three of these genes have been implicated in the process of cyst formation.[25–27] We propose that reduced expression of *Pkd2* and *Tsc1* at later stages may further contribute to the observed phenotype. The tuberous sclerosis complex gene *Tsc1*, also known as hamartin, has many functions but particularly is involved in regulating mammalian target of rapamycin complex 1 signaling, which has been a target of inhibiting human ADPKD progression.[35]

In conclusion, our findings demonstrate that Grhl2 modulates the progression of collecting duct–derived cysts, providing potential segment-specific understanding for further treatment opportunities to slow or halt cyst progression in PKD.

Disclosures

Disclosure forms, as provided by each author, are available with the online version of the article at http://links.lww.com/JSN/E645.

Funding

K.M. Schmidt-Ott: Deutsche Forschungsgemeinschaft (SFB 1365, GRK 2318, and FOR 2841). P. Boor: European Research Council (No 101001791), Bundesministerium für Bildung und Forschung (BMBF, STOP-FSGS-01, GM1901A), Deutsche Forschungsgemeinschaft (322900939, 454024652, 432698239, and 445703531), and Federal Ministry of Education and Research (BMBF, STOP-FSGS-01GM1901A). Z.Y. Yurtdas: Urological Research Foundation, Berlin (stipend).

Acknowledgments

We thank Prof. Dr. Friedrich C. Luft and Dr. Atakan Aydin for critical comments and suggestions regarding the manuscript; Dr. Anje Sporbert and Matthias Richter (Max Delbrück Center; Advanced Light Microscopy Facility) for providing technical expertise in confocal microscopy. We also thank Gabriel Kirchgraber, Tatjana Luganskaja, Loreen Kabuß, Anna Maren Maier, and Siegrun Blauhut for their excellent technical support. This study was part of Z.Y. Yurtdas's doctoral thesis, which was submitted to Humboldt University Berlin, Germany in September 2019.

Author Contributions

Conceptualization: Kai M. Schmidt-Ott, Zeliha Yesim Yurtdas.
Methodology: Peter Boor, Klaus Jung, Ergin Kilic, Markus Landthaler, Kai M. Schmidt-Ott, Emanuel Wyler, Zeliha Yesim Yurtdas.
Validation: Zeliha Yesim Yurtdas.
Visualization: Zeliha Yesim Yurtdas.
Writing – original draft: Zeliha Yesim Yurtdas.
Writing – review & editing: Kai M. Schmidt-Ott, Zeliha Yesim Yurtdas.

Data Sharing Statement

All data are included in the manuscript and/or supporting information.

Supplemental Material

This article contains the following supplemental material online at http://links.lww.com/JSN/E644.

Supplemental Figure 1. Reanalysis of RNA-seq data using Hisat2.

Supplemental Figure 2. Full scans of Western blots and band density analysis.

Supplemental Figure 3. Immunohistochemical staining for c-MYC and Grhl2 in kidney samples from 10-week-old control and TCKD mice.

Supplemental Figure 4. Real-time quantitative PCR validation of differentially expressed genes identified by RNA-seq.

Supplemental Table 1. Primer list for genotyping.

Supplemental Table 2. Primary antibody list.

Supplemental Table 3. Secondary antibody list.

Supplemental Table 4. RT-PCR primer list.

References

1. Kim B, King BF Jr., Vrtiska TJ, Irazabal MV, Torres VE, Harris PC. Inherited renal cystic diseases. *Abdom Radiol (NY).* 2016;41(6):1035–1051. doi:10.1007/s00261-016-0754-3
2. Ward CJ, Hogan MC, Rossetti S, et al. The gene mutated in autosomal recessive polycystic kidney disease encodes a large, receptor-like protein. *Nat Genet.* 2002;30(3):259–269. doi:10.1038/ng833
3. Torres VE, Harris PC, Pirson Y. Autosomal dominant polycystic kidney disease. *Lancet.* 2007;369(9569):1287–1301. doi:10.1016/S0140-6736(07)60601-1
4. Grantham JJ. Clinical practice. Autosomal dominant polycystic kidney disease. *N Engl J Med.* 2008;359(14):1477–1485. doi:10.1056/NEJMcp0804458
5. Mehta YR, Lewis SA, Leo KT, et al. "ADPKD-omics": determinants of cyclic AMP levels in renal epithelial cells. *Kidney Int.* 2022;101(1):47–62. doi:10.1016/j.kint.2021.10.014
6. Lanktree MB, Haghighi A, di Bari I, Song X, Pei Y. Insights into autosomal dominant polycystic kidney disease from genetic studies. *Clin J Am Soc Nephrol.* 2021;16(5):790–799. doi:10.2215/CJN.02320220
7. Werth M, Walentin K, Aue A, et al. The transcription factor grainyhead-like 2 regulates the molecular composition of the epithelial apical junctional complex. *Development.* 2010;137(22):3835–3845. doi:10.1242/dev.055483
8. Walentin K, Hinze C, Werth M, et al. A Grhl2-dependent gene network controls trophoblast branching morphogenesis. *Development.* 2015;142(6):1125–1136. doi:10.1242/dev.113829
9. Aue A, Hinze C, Walentin K, et al. A grainyhead-like 2/ovo-like 2 pathway regulates renal epithelial barrier function and lumen expansion. *J Am Soc Nephrol.* 2015;26(11):2704–2715. doi:10.1681/ASN.2014080759
10. Hinze C, Ruffert J, Walentin K, et al. GRHL2 is required for collecting duct epithelial barrier function and renal osmoregulation. *J Am Soc Nephrol.* 2018;29(3):857–868. doi:10.1681/ASN.2017030353
11. Boivin FJ, Schmidt-Ott KM. Functional roles of Grainyhead-like transcription factors in renal development and disease. *Pediatr*

Nephrol. 2020;35(2):181–190. doi:10.1007/s00467-018-4171-4
12. Olesen ETB, Fenton RA. Aquaporin 2 regulation: implications for water balance and polycystic kidney diseases. *Nat Rev Nephrol.* 2021;17(11):765–781. doi:10.1038/s41581-021-00447-x
13. Sander S, Calado DP, Srinivasan L, et al. Synergy between PI3K signaling and MYC in Burkitt lymphomagenesis. *Cancer Cell.* 2012;22(2):167–179. doi:10.1016/j.ccr.2012.06.012
14. Dodt M, Roehr JT, Ahmed R, Dieterich C. FLEXBAR-flexible barcode and adapter processing for next-generation sequencing platforms. *Biology (Basel).* 2012;1(3):895–905. doi:10.3390/biology1030895
15. Love MI, Huber W, Anders S. Moderated estimation of fold change and dispersion for RNA-seq data with DESeq2. *Genome Biol.* 2014;15(12):550. doi:10.1186/s13059-014-0550-8
16. Gaidatzis D, Lerch A, Hahne F, Stadler MB. QuasR: quantification and annotation of short reads in R. *Bioinformatics.* 2015;31(7):1130–1132. doi:10.1093/bioinformatics/btu781
17. Goldman MJ, Craft B, Hastie M, et al. Visualizing and interpreting cancer genomics data via the Xena platform. *Nat Biotechnol.* 2020;38(6):675–678. doi:10.1038/s41587-020-0546-8
18. Grantham JJ, Geiser JL, Evan AP. Cyst formation and growth in autosomal dominant polycystic kidney disease. *Kidney Int.* 1987;31(5):1145–1152. doi:10.1038/ki.1987.121
19. Lanoix J, D'Agati V, Szabolcs M, Trudel M. Dysregulation of cellular proliferation and apoptosis mediates human autosomal dominant polycystic kidney disease (ADPKD). *Oncogene.* 1996;13(6):1153–1160. PMID: 8808689
20. Trudel M, D'Agati V, Costantini F. c-myc as an inducer of polycystic kidney disease in transgenic mice. *Kidney Int.* 1991;39(4):665–671. doi:10.1038/ki.1991.80
21. Trudel M, Barisoni L, Lanoix J, D'Agati V. Polycystic kidney disease in SBM transgenic mice: role of c-myc in disease induction and progression. *Am J Pathol.* 1998;152(1):219–229. PMID: 9422539
22. Traykova-Brauch M, Schonig K, Greiner O, et al. An efficient and versatile system for acute and chronic modulation of renal tubular function in transgenic mice. *Nat Med.* 2008;14(9):979–984. doi:10.1038/nm.1865
23. Huang DW, Sherman BT, Lempicki RA. Bioinformatics enrichment tools: paths toward the comprehensive functional analysis of large gene lists. *Nucleic Acids Res.* 2009;37(1):1–13. doi:10.1093/nar/gkn923
24. Huang DW, Sherman BT, Lempicki RA. Systematic and integrative analysis of large gene lists using DAVID bioinformatics resources. *Nat Protoc.* 2009;4(1):44–57. doi:10.1038/nprot.2008.211
25. Jadeja S, Smyth I, Pitera JE, et al. Identification of a new gene mutated in Fraser syndrome and mouse myelencephalic blebs. *Nat Genet.* 2005;37(5):520–525. doi:10.1038/ng1549
26. Kirby A, Gnirke A, Jaffe DB, et al. Mutations causing medullary cystic kidney disease type 1 lie in a large VNTR in MUC1 missed by massively parallel sequencing. *Nat Genet.* 2013;45(3):299–303. doi:10.1038/ng.2543
27. Latres E, Malumbres M, Sotillo R, et al. Limited overlapping roles of P15(INK4b) and P18(INK4c) cell cycle inhibitors in proliferation and tumorigenesis. *EMBO J.* 2000;19(13):3496–3506. doi:10.1093/emboj/19.13.3496
28. Schonauer R, Baatz S, Nemitz-Kliemchen M, et al. Matching clinical and genetic diagnoses in autosomal dominant polycystic kidney disease reveals novel phenocopies and potential candidate genes. *Genet Med.* 2020;22(8):1374–1383. doi:10.1038/s41436-020-0816-3
29. Wilson PD. Mouse models of polycystic kidney disease. *Curr Top Dev Biol.* 2008;84:311–350. doi:10.1016/S0070-2153(08)00606-6
30. Lu W, Fan X, Basora N, et al. Late onset of renal and hepatic cysts in Pkd1-targeted heterozygotes. *Nat Genet.* 1999;21(2):160–161. doi:10.1038/5944
31. Boulter C, Mulroy S, Webb S, Fleming S, Brindle K, Sandford R. Cardiovascular, skeletal, and renal defects in mice with a targeted disruption of the Pkd1 gene. *Proc Natl Acad Sci U S A.* 2001;98(21):12174–12179. doi:10.1073/pnas.211191098
32. Lantinga-van Leeuwen IS, Leonhard WN, van der Wal A, Breuning MH, de Heer E, Peters DJM. Kidney-specific inactivation of the Pkd1 gene induces rapid cyst formation in developing kidneys and a slow onset of disease in adult mice. *Hum Mol Genet.* 2007;16(24):3188–3196. doi:10.1093/hmg/ddm299
33. Koslowski S, Latapy C, Auvray P, Blondel M, Meijer L. An overview of in vivo and in vitro models for autosomal dominant polycystic kidney disease: a journey from 3D-cysts to mini-pigs. *Int J Mol Sci.* 2020;21(12):4537. doi:10.3390/ijms21124537
34. Hinze C, Karaiskos N, Boltengagen A, et al. Kidney single-cell transcriptomes predict spatial corticomedullary gene expression and tissue osmolality gradients. *J Am Soc Nephrol.* 2021;32(2):291–306. doi:10.1681/ASN.2020070930
35. Walz G, Budde K, Mannaa M, et al. Everolimus in patients with autosomal dominant polycystic kidney disease. *N Engl J Med.* 2010;363(9):830–840. doi:10.1056/NEJMoa1003491